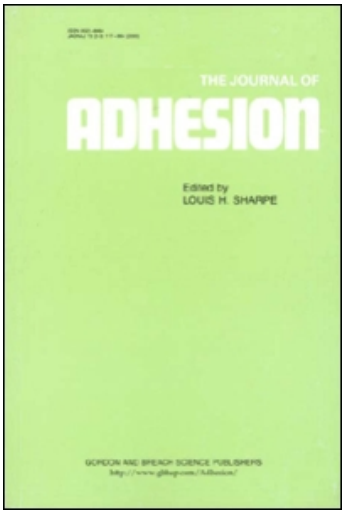

The Journal of Adhesion

Publication details, including instructions for authors and subscription information:
http://www.informaworld.com/smpp/title~content=t713453635

Experimental Study of Fibrin Embolization Under Shear Flow

Sylvie Lorthois; Philippe Schmitz[a]; Didier Houi[a]; Eduardo Angles-cano[b]
[a] Institut de Mécanique des Fluides de Toulouse, Toulouse Cedex, France [b] INSERM U. 143 "Hémostase et Biologie Vasculaire", Bicêtre, France

To cite this Article Lorthois, Sylvie , Schmitz, Philippe , Houi, Didier and Angles-cano, Eduardo(2000) 'Experimental Study of Fibrin Embolization Under Shear Flow', The Journal of Adhesion, 72: 2, 229 — 239
To link to this Article: DOI: 10.1080/00218460008029280
URL: http://dx.doi.org/10.1080/00218460008029280

J. Adhesion, 2000, Vol. 72, pp. 229 - 239
Reprints available directly from the publisher
Photocopying permitted by license only

Experimental Study of Fibrin Embolization Under Shear Flow*

SYLVIE LORTHOIS[a,†], PHILIPPE SCHMITZ[a], DIDIER HOUI[a] and EDUARDO ANGLES-CANO[b]

[a] *Institut de Mécanique des Fluides de Toulouse, UMR CNRS 5502, Allées du Professeur Camille Soula, 31400 Toulouse Cedex, France;*
[b] *INSERM U. 143 "Hémostase et Biologie Vasculaire", 84, rue du Général Leclerc, 94276-Cedex, Bicêtre, France*

(Received 7 June 1999 ; In final form 22 October 1999)

Arterial thrombi consist mainly of platelets and fibrin, the biopolymer produced in the final step of the coagulation cascade. Thrombus fragmentation may result in occlusion of smaller distal vessels (embolization), a serious and often fatal event. The objective of this study is to investigate the role of the fibrin polymer network on the resistance of a clot to fragmentation under shear flow. For that purpose, a fibrin clot model representative of native clots is submitted to a shear flow that reproduces the pathophysiological range of shear stress.

The adhesion force due to specific fibrin/fibrin interactions is determined from the measurement of the shear stress producing 50% detachment of model particles of blood platelets embedded in the clot. This force was found to be several orders higher than the nonspecific colloidal forces between surfaces, which can, thus, be neglected. Influence of the number of fibrin monolayers in the clot model on adhesion force is investigated.

Keywords: Bioadhesion; particle detachment; fibrin; shear; clot model; flow chamber

1. INTRODUCTION

The central event in the blood coagulation process is the thrombin-catalyzed conversion of soluble fibrinogen into insoluble fibrin, *i.e.*,

* Presented at the 22nd Annual Meeting of The Adhesion Society, Inc., Panama City Beach, Florida, USA, February 21–24, 1999.

†Corresponding author. Tel.: 33-(0)5-61-28-58-77, Fax: 33-(0)5-61-28-58-78, e-mail: lorthois@imft.fr

formation of fibrin monomers followed by non-covalent self-assembly of monomeric fibrin units into a three-dimensional meshwork [1]. This meshwork provides structural support for arterial thrombi (mainly constituted of platelets and fibrin) and appears to be one of the major factors that controls their stability [2].

Thrombus fragmentation may result in occlusion of smaller distal vessels (embolization) producing ischemia, a serious and often fatal event. In particular, it has been shown that a mural thrombus is the main source of downstream cerebral microemboli in patients with high-grade internal carotid artery stenosis [3]. An attracting hypothesis is that the fragmentation of an arterial thrombus may be related not only to the biochemical structure of the thrombus, but also to physical properties of the blood flow such as the local shear stress acting on the thrombus [4].

Therefore, the objective of this study was to investigate the role of the fibrin polymer meshwork on the resistance of thrombi to fragmentation under shear flow, with the use of a hydrodynamic method [5].

2. METHODOLOGY

The experimental methodology is based on the association of a fibrin clot model [6] and a controlled-shear flow chamber that reproduces the pathophysiological range of shear stresses.

2.1. Fibrin Clot Model (Fig. 1)

The fibrin clot model consist of a predefined number of fibrin molecular monolayers covalently bound to an amino-modified glass plate, and of model particles of blood platelets (fibrin-coated amino-modified latex beads, 2 μm diameter, Interfacial Dynamics Corporation, Portland, OR USA).

Amino-modified glass is first prepared by incubation of (3-aminopropyl)diethoxymethylsilane (1% v/v in anhydrous toluene) with glass under nitrogen [7]. After silanization, human fibrinogen is coupled to the glass and to the amino-modified latex-beads by means of polyglutaraldehyde chemistry [6]. The fibrinogen monolayer

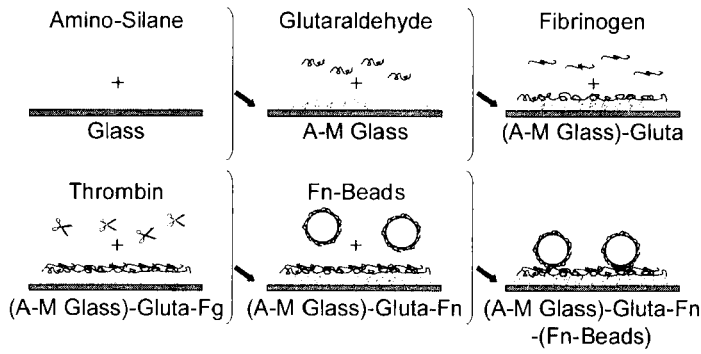

FIGURE 1 Fibrin clot model preparation. A-M Glass: Amino-modified glass, Gluta: Glutaraldehyde, Fg: Fibrinogen, Fn: fibrin. Products are incubated with the surface, and rinsed before next step.

covalently bound to the surfaces is transformed into a fibrin monolayer by treatment with thrombin [8]. Additional layers can be added to the initial one by experimental reproduction of the steps of heterogeneous catalysis at the fibrin/blood interface; fibrinogen is first incubated with the previous fibrin layer, and the bound fibrinogen is transformed into fibrin. Finally, the model particles of platelets (fibrin monolayer coated amino-modified latex beads) are allowed to settle under gravity on the fibrin surface.

2.2. Shear Stress Flow Chamber (Fig. 2)

The chamber is composed of a bottom glass plate onto which is prepared the fibrin clot model and of an upper Plexiglas plate pierced for the entry and the exit of fluid and for the injection of latex beads; these plates are separated by a hollowed steel plate for channeling the fluid flow (respective thickness: 4, 10 and 0.2 mm). All the plates are held together with aluminium clamps. The rectangular flow channel (10 mm width) follows a diverging-converging channel, in order to ensure a uniform flow at the entrance.

The chamber is mounted on the stage of an inverted microscope (NIKON Diaphot), coupled to a CCD camera with a video image-processing system for visualization and counting of particles. The observation area is located far downstream of the rectangular channel entry, in order to avoid entrance effects.

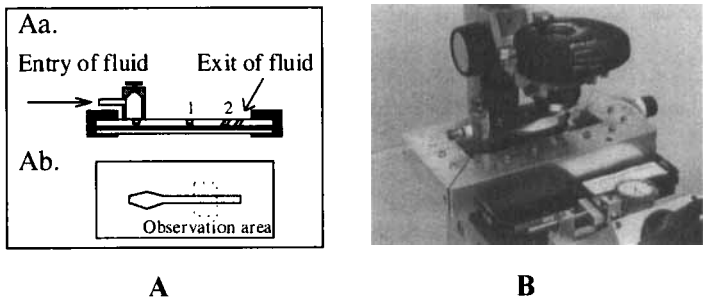

FIGURE 2 Shear Stress Flow Chamber. A: Schematic view of the chamber (a: side view, b: upper view of the hollowed steel plate) 1, upstream pressure tap; 2, downstream pressure tap or particle-injection tap. B: Position on the stage of the inverted microscope.

2.3. Flow Characteristics

A laminar unidirectional Poiseuille flow in the observation area is obtained. Indeed, the theoretical relation between pressure drop (ΔP) and flow rate (Q) for plane two-dimensional Poiseuille flows:

$$\frac{\Delta P}{\mu Q} = \frac{12 \cdot \Delta x}{h^3 \cdot l} \tag{1}$$

where μ is the dynamic viscosity, Δx the distance between the pressure taps, and h and l the height and width of the flow channel, respectively, was experimentally verified (Fig. 3). The relationship

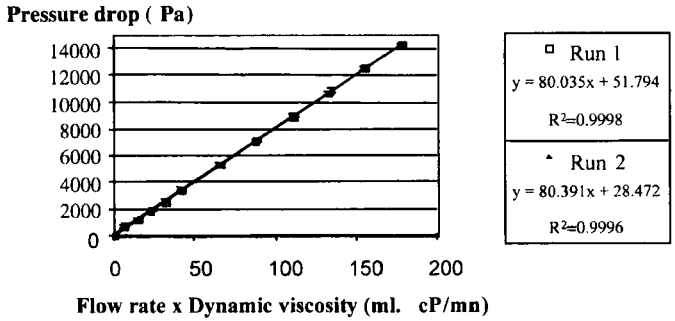

FIGURE 3 Experimental relation between pressure drop and flow rate × dynamic viscosity. Experimental relationship is linear, up to the greatest flow rates, demonstrating the non-deformation of the flow chamber at high pressures. The slope of the curve gives an effective value for h of 208.8 mm ± 0.8% (specified value of 200 mm ± 5%).

obtained is linear, up to the greatest flow rates, proving the non-deformation of the flow chamber at high pressures. The slope of the curve gives an effective value for h of 208.8 mm ± 0.8% (specified value of 200 mm ± 5%).

For this type of flow, the wall shear stress, τ_w, is uniform except in a short entry zone the length of which is about $0.06(\rho hQ/\mu l)$, where ρ is the fluid density, and in areas 1 mm in width near the channel side walls. Outside, τ_w is given by:

$$\tau_w = \frac{6 \cdot \mu \cdot Q}{h^2 \cdot l} \tag{2}$$

The pathophysiological range of shear stresses (1 to 60 Pa) [9] is obtained for flow rates between 4 and 240 ml/mn.

The channel height being large compared with the latex-bead size, the bead size large compared with the surface rugosity of the fibrin meshwork (about 2 nanometers from AFM investigations) and the particulate Reynolds number negligible, the flow in the particle vicinity is a creeping linear shear flow. The hydrodynamic force exerted on a bead is parallel to the flow direction and is given by O'Neil [10]:

$$F_h = 32.00 \cdot r_b^2 \cdot \tau_w \tag{3}$$

where r_b is the bead radius. This expression, determined for a single sphere in contact with a plane wall in an infinite linear shear flow, is valid for an array of beads that are adherent to the bottom plate of a flow channel, if the bead radius is less than (1/15) of the gap thickness [11] and if their separation distance is larger than 10 times the bead radius [5].

2.4. Procedure for Particle Detachment Experiments

The bottom glass plate of the chamber is first coated with fibrin, then the chamber is assembled, placed on the stage, and filled with buffer (sodium phosphate 0.05 M, pH = 7.4, NaCl 0.08 M, NaN_3 0.01%). Fibrin-coated latex beads ($\approx 10^7$ beads/ml) are slowly injected into the flow chamber through a syringe valve, and are allowed to settle under gravity, resulting in bead separation distances between 5 and 10 bead diameters. This separation distance was chosen to minimize

artifacts caused by hydrodynamic interactions between particles, such as shielding of the shear field [5]. The beads are then incubated with the coated surface for 14 hours, and the flow rate is increased step by step (a typical step is three minutes, see Section 3.2). At the end of each step, the number of particles remaining at the glass surface, as a function of shear stress applied, is counted by the means of phase-contrast optical microscopy and image acquisition/treatment. When the maximal flow rate is reached, flow is stopped and a last flush at maximal flow rate is performed, in order to assess the role of transitory effects.

The same procedure is applied to bare particles upon a bare glass surface in order to evaluate the contribution of non-specific adhesion forces (*i.e.*, DLVO forces [13]) to the total adhesion.

3. RESULTS AND DISCUSSION

3.1. Fibrin Clot Model

The different steps of the fabrication of the fibrin clot model were characterized with the use of monoclonal antibodies as described in Ref. [8]. Briefly, the transformation of fibrinogen into fibrin monomers is quantitatively measured by the decrease in reactivity of Y18, an antibody that specifically recognizes the fibrinopeptide A of fibrinogen cleaved by thrombin (Fig. 4).

The formation of polymerized fibrin is proven by the increase in reactivity of DDi2F7, a monoclonal that specifically recognizes the D-dimers of fibrin produced by the self-assembly of two fibrin

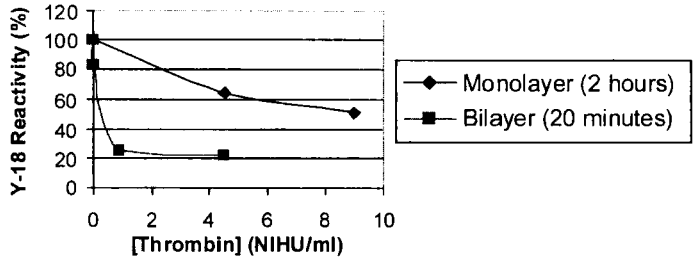

FIGURE 4 Relation between Y-18 reactivity and thrombin concentration. Relation between Y-18 reactivity and thrombin concentration in two different systems: a fibrinogen monolayer (thrombin incubation time: 2 hours), and a fibrinogen monolayer bound to a fibrin monolayer (thrombin incubation time: 20 minutes).

monomers. The ability of the fibrin meshwork to bind plasminogen and its activator (*t*-PA) specifically, in a dose-dependent and saturating manner, with a high affinity, indicates that fibrin thus produced is functionally representative of native clots.

3.2. Detachment Experiments

In order to validate the experimental technique, we first studied the time dependence of the detachment of bare beads in contact with a bare glass surface under a constant flow rate. The evolution of the number of particles remaining in the observation area (expressed as the percentage of the initial number of particles) as a function of time of application of a constant flow rate is plotted in Figure 5. It can be seen that the number of particles remaining at the glass surface stays unchanged after a step of three minutes. Subsequently, the further detachment experiments are performed with flow rate steps of three minutes.

After each experiment, results obtained were checked as follows: the number of particles remaining in both half observation areas at each flow rate step were plotted as a function of the number of particles remaining in the whole observation area (see Fig. 6). In the ideal case (no variability of bead radius, perfect contact area....), the curve obtained should be the first bisecting line. However, the bead size is distributed (coefficient of variation of diameter: 6.1%) and the number of particles initially present in the area is finite (40 to 200). Therefore, results were eliminated in some cases when the deviation from the bisecting line was greater than 20%.

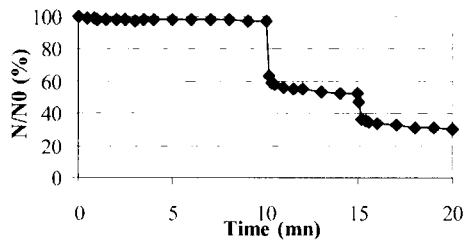

FIGURE 5 Relation between number of bare latex particles remaining at bare glass surface in the observation area (expressed as percent of initial number of particles) and time. Flow rate is increased step-by-step: $T = 0$, $Q = 1$ ml/mn; $T = 10$, $Q = 4.5$ ml/mn; $T = 15$, $Q = 8$ ml/mn.

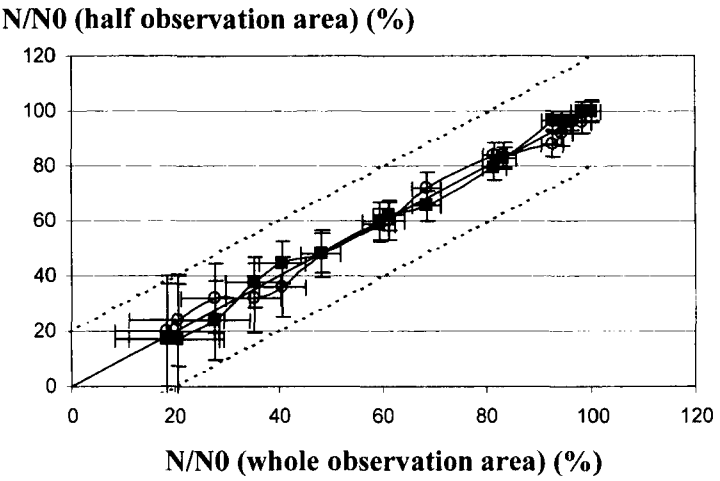

FIGURE 6 Number of particles remaining in both half observation areas *versus* number of particles remaining in the whole observation area. Initial number of fibrin-coated beads in contact with a fibrin monolayer: 54.

To evaluate the specific adhesion force due to fibrin/fibrin interactions, detachment experiments were carried out for three different systems: bare latex beads in contact with bare glass, fibrin-coated beads in contact with a fibrin monolayer and fibrin-coated beads in contact with a fibrin bilayer. The results are presented in Figure 7.

Firstly, we can observe that the evolution of bead detachment when specific fibrin/fibrin interactions take place is significantly different, compared with the case where only non-specific DLVO forces exist. In the latter case, there is no shear-rate threshold below which the flow cannot overcome adhesion forces. The non-specific DLVO interaction is, therefore, very weak (similar results were obtained with fibrin-coated beads upon a bare glass surface: data not shown).

Secondly, the adhesion force appears to be drastically increased in the presence of the fibrin meshwork. Moreover, a shear rate threshold is evidenced: about 1 Pa for the interaction fibrin-coated beads/fibrin monolayer, and about 10 Pa for the interaction fibrin-coated beads/fibrin bilayer, which corresponds to a drag force $F_h \sim 32$ pN, and $F_h \sim 320$ pN, respectively. In addition, at the end of the experiment, 20% to 40% of the initial coated beads remain attached to the ground of the chamber, whereas more than 99% of the bare beads

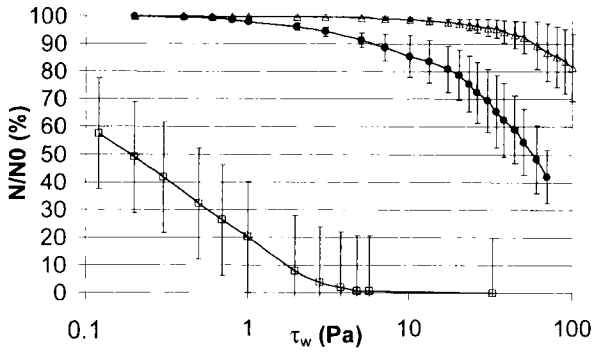

FIGURE 7 Number of particles remaining in the observation area (expressed as percent of initial number of particles) *versus* wall shear stress. □: detachment of bare particles from bare glass ($n = 9$); •: detachment of fibrin-coated particles from fibrin monolayer ($n = 2$); Δ: detachment of fibrin-coated particles from fibrin bilayer ($n = 4$). Results are displayed as mean ± SD of n experiments conduced either in quadruplicates or in quintuplicates, except for the detachment of bare particles from bare glass where independent experiments where conduced with one single sample. ([1]By independent experiments, we mean experiments performed with fibrin surfaces prepared independently. The term "quadruplicates" is slightly different than in the current meaning. Four samples (fibrin-coated glass and beads) prepared simultaneously are submitted independently to the detachment experiments.)

are detached. The last flush at maximal flow rate has no further influence, showing the negligible action of transitory effects.

Adhesion of fibrin-coated beads is further enhanced in the presence of a fibrin bilayer compared with a fibrin monolayer: a shear stress of 50 Pa is sufficient to obtain the detachment of 50% of beads in the monolayer system, while such a shear stress is able to remove less than 20% of beads in the bilayer system. The effect of the bilayer can be explained as follows. Firstly, the structure of the upper fibrin layer is probably closer to the physiologic structure in the bilayer system, thus allowing a better exposure of the polymerization sites. Secondly, the contact area is probably enhanced, due to the greater thickness of the fibrin bilayer [12].

4. CONCLUSION AND PERSPECTIVES

Promising results concerning the adhesion forces due to specific fibrin/fibrin interactions were obtained. The effect of biochemical

conditions of fibrin formation on adhesion force have to be further investigated. In particular, the effect of plasmin, the main physiological fibrinolytic enzyme, that digests the fibrin network, may produce an important decrease of the adhesion force.

A force and torque balance, taking into account the role of viscoelasticity of fibrin/fibrin bonds, has to be performed in order to obtain quantitative information about the adhesive contribution of the fibrin polymer. In addition, the results have also to be compared with the pathophysiological shear stress values, in order to improve the knowledge on the mechanisms of arterial thrombo-embolism.

Acknowledgments

We would like to thank Dr. Marc-Vergnes and Dr. Cassot for their active collaboration, Dr. Coratger for his expertise in AFM, and F. Esteban and S. Loyau for valuable technical assistance. Financial support from the INSERM (Intercommission No. 1 grant 4M101C) and from the CNRS is gratefully acknowledged.

References

[1] Mossesson, M. W., "The assembly and structure of the fibrin clot", *Nouv. Rev. Fr. Hematol.* **34**, 11 (1992).
[2] Blomback, B., "Fibrinogen and fibrin: proteins with complex roles in hemostasis and thrombosis", *Throm. Res.* **83**, 1 (1996).
[3] Sitzer, M., Müller, W., Siebler, M., Hort, W., Kniemeyer, H. W., Jäncke, L. and Steinmetz, H., "Plaque ulceration and lumen thrombus are the main sources of cerebral microemboli in high-grade internal carotid artery stenosis", *Stroke* **26**, 1231 (1995).
[4] Sakariassen, K. S. and Barstad, R. M., "Mechanisms of thromboembolism at arterial plaques", *Blood Coag. Fibrinol.* **4**, 615 (1993).
[5] Elzo, D., Schmitz, P., Houi, D. and Joscelyne, S., "Measurement of particle/membrane interaction by a hydrodynamic method", *J. Membrane Sci.* **109**, 43 (1996).
[6] Anglés-Cano, E. A., "Spectrophotometric solid-phase fibrin-tissue plasminogen activator activity assay (SOFIA-tPA) for high-fibrin-affinity tissue plasminogen activators", *Anal. Biochem.* **153**, 201 (1986).
[7] J., Ho Moon, Shin, J., Kim, S. and Park, J., "Formation of uniform aminosilane thin layers: an imine formation to measure relative surface density of the amine group", *Langmuir* **12**, 4621 (1996).
[8] Fleury, V. and Anglés-Cano, E., "Characterization of the binding of plasminogen to fibrin surfaces: the role of carboxy-terminal lysines", *Biochemistry* **30**, 7630 (1991).
[9] Lorthois, S., Cassot, F. and Marc-Vergnes, J. P., "Taux de cisaillement pariétal maximal dans une sténose carotidienne et fonctionnalité du cercle de Willis", *Arch. Physiol. Biochem.* **106(B)**, 111 (1998).

[10] O'Neil, M. E., "A sphere in contact with a plane wall in a slow linear shear flow", *Chem. Eng. Sci.* **23**, 1293 (1968).
[11] Brooks, S. B. and Tozeren, A., "Flow past an array of cells that are adherent to the bottom plate of a flow channel", *Comp. and Fluids* **25**, 741 (1996).
[12] Cozens-Roberts, C., Quinn, J. and Lauffenburger, D., "Receptor mediated adhesion phenomena", *Biophys. J.* **58**, 107 (1990).
[13] Israelachvili, J., "Intermolecular and Surface Forces" (Academic Press, NY, 1992), p. 246.